Journal of Zhejiang University SCIENCE A
ISSN 1673-565X (Print); ISSN 1862-1775 (Online)
www.zju.edu.cn/jzus; www.springerlink.com
E-mail: jzus@zju.edu.cn

Measurement of the thermal transport properties of dielectric thin films using the micro-Raman method*

Shuo HUANG, Xiao-dong RUAN, Xin FU†‡, Hua-yong YANG

(*State Key Laboratory of Fluid Power Transmission and Control, Zhejiang University, Hangzhou 310027, China*)

†E-mail: xfu@zju.edu.cn

Received June 27, 2008; Revision accepted Sept. 25, 2008; Crosschecked Oct. 29, 2008

Abstract: The micro-Raman method is a non-contact and non-destructive method for thermal conductivity measurement. To reduce the measurement error induced by the poor fit of the basic equation of the original micro-Raman method, we developed a new basic equation for the heat source of a Gaussian laser beam. Based on the new basic equation, an analytical heat transfer model has been built to extend the original micro-Raman method to thin films with submicrometer- or nanometer-scale thickness. Experiments were performed to measure the thermal conductivity of dielectric thin films with submicrometer- or nanometer-scale thickness. The thermal resistance of the interface between dielectric thin films and their silicon substrate was also obtained. The obtained thermal conductivity of silicon dioxide film is 1.23 W/(m·K), and the interface thermal resistance between silicon dioxide film and substrate is 2.35×10^{-8} m^2·K/W. The thermal conductivity and interface thermal resistance of silicon nitride film are 1.07 W/(m·K) and 3.69×10^{-8} m^2·K/W, respectively. The experimental results are consistent with reported data.

Key words: Thermal conductivity, Dielectric thin films, Submicrometer- or nanometer-scale, Porous silicon, Thermal effect micro-systems (TEMS)

doi:10.1631/jzus.A0820493 **Document code:** A **CLC number:** O55; TN3

INTRODUCTION

Heat transfer plays an important role in the performance of thermal effect micro-systems (TEMS). The operating principles of typical TEMS, such as infra-red detectors and thermal flow sensors, require a reliable thermal insulation of the sensing elements from the silicon substrate. This improves the measurement accuracy by reducing the impact of heat dissipation in the silicon substrate (Perichon *et al.*, 2000). Until now, two main methods were used to ensure the thermal isolation of TEMS. The first method was to use microstructures: thin silicon microstructures can be micromachined in bulk silicon such as cantilever beams or membranes with high thermal resistance but poor mechanical stability (Chen *et al.*, 2005; Bruschi *et al.*, 2006). The second method relates to materials: materials with thermal conductivity can be applied as a part of the substrate (Kaltsas and Nassiopoulou, 1999; Bruschi *et al.*, 2006). Porous silicon, as a material with much lower thermal conductivity than monocrystalline silicon and more mechanical stability than thin silicon microstructures, can be applied to the thermal insulation of TEMS (Dominguez *et al.*, 1993; Kaltsas and Nassiopoulou, 1999; Kan and Finstad, 2005). Dielectric thin films like silicon dioxide and silicon nitride films are commonly used as dielectric and passivation layers in TEMS and integrated circuits (IC) for their excellent physical and electronic properties (Lee and Cahill, 1997). The thermal properties of porous silicon and dielectric thin films are crucial for the performance of the TEMS and IC. To evaluate the heat dissipation in porous silicon and dielectric thin films, it is very important to investigate their thermal conductivity. A measurement

‡ Corresponding author

* Project supported by the State Key Program of National Natural Science Foundation of China (No. 50335010), and the Zhejiang Provincial Natural Science Foundation (No. R105008), China

method is then required to obtain the thermal conductivity of porous silicon and dielectric thin films.

Several methods for measuring film thermal conductivity have been reported, such as the steady-state method (Zhang and Gridgoropoulos, 1995), the 3ω method (Cahill *et al*., 1994), the photoacoustic method (Swimm, 1983), the thermo-reflectance method (Burzo *et al*., 2002; Komarov *et al*., 2003), and the thermal microscopy method (Callard *et al.*, 1999). Both the steady-state and 3ω methods require depositing a metal layer on the measured film, which may risk damaging and changing the properties of the measured film. Photoacoustic and thermal-reflectance methods are non-contact but indirect methods requiring extensive data analysis. The thermal microscopy method uses a probe as a key component but the fabrication process of the probe is very complicated.

Perichon *et al*.(1999) measured the thermal conductivity of porous silicon using the micro-Raman method. They used a new thermal conductivity measurement method with micro-Raman spectroscopy by combining the effect of the temperature-dependent Raman peak shift (Tsu and Hernandez, 1982) with the basic equation of the thermal scanning probe microscopy method (Nonnenmacher and Wickramasinghe, 1992). Because the heat sources in the two methods are different, the basic equation from the thermal scanning probe microscopy method cannot be applied to the micro-Raman method.

To reduce the measurement error induced by the unsuitability of the equation, in this paper, a new basic equation is derived for the heat source of a Gaussian laser beam to express the relationship between the thermal conductivity and the laser-induced local temperature rise. With the new basic equation, experiments were performed to measure the thermal conductivity of porous silicon films.

Furthermore, according to Perichon *et al*.(1999), the micro-Raman method cannot calculate the thermal conductivity of thin films with submicrometer- or nanometer-scale thickness, because the thickness of the film sample is required to be larger than the laser beam diameter. The laser beam diameter of the micro-Raman device is from several to tens of micrometers.

To extend the micro-Raman method to the thermal conductivity measurement of thin films with submicrometer- or nanometer-scale thickness, an analytical heat transfer model was developed based on the new basic equation. The model uses thermal resistance to describe the effects of thin film thickness and thermal conductivity of thin film and substrate. By using the extended micro-Raman method, experiments were performed to measure the thermal conductivity of submicrometer- and nanometer-scale thickness dielectric thin films. The interface thermal resistance between dielectric thin films and silicon substrate was also obtained.

ANALYSIS OF THE HEAT TRANSFER

Fig.1 shows a Gaussian laser beam irradiating a sample which consists of a substrate and a film of thickness, δ. The centre of the laser beam on the film sample surface is taken as the origin of the cylindrical coordinate system (r, z).

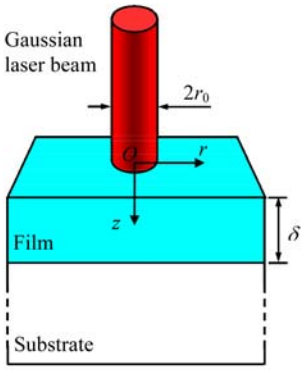

Fig.1 Film and substrate in cylindrical coordinate system (r, z)

The intensity of the Gaussian laser beam is

$$I(r)=\frac{2P}{\pi r_0^2}\exp\left(-\frac{2r^2}{r_0^2}\right), \tag{1}$$

where P is the power of the laser beam, r_0 is the radius at which the laser beam intensity is e^{-2} times its maximum value.

Heat transfer in thick film induced by a Gaussian laser beam

Consider a Gaussian laser beam that induces

shallow heating on a relatively thick film sample, and where the thickness of the film is larger than the diameter of the laser beam. In this approximate analysis, it is assumed that the laser beam power is completely absorbed by the film sample (Perichon *et al.*, 1999), and the heat losses in the air are negligible when the airflow around the film sample remains still. The problem then reduces to the steady-state case of heat flow transfer into a semi-infinite half-space from a circular region on the surface of this half-space. The temperature $t(r, z)$ in the film sample then satisfies the equation:

$$\frac{\partial^2 t(r,z)}{\partial r^2}+\frac{1}{r}\frac{\partial t(r,z)}{\partial r}+\frac{\partial^2 t(r,z)}{\partial z^2}=0. \tag{2}$$

The boundary condition is

$$\frac{\partial t(r,z)}{\partial z}=f(r)=-\frac{I(r)}{k}=-\frac{2P}{k\pi r_0^2}\exp\left(-\frac{2r^2}{r_0^2}\right),$$
$$\text{at } 0<r<r_0,\ z=0, \tag{3}$$

where k is the thermal conductivity of the film sample. It is assumed that as $(r^2+z^2)^{1/2}\to\infty$, $t(r, z)\to 0$.

By taking the Hankel transform of order zero, Eq.(2) turns to

$$\frac{\mathrm{d}^2 T(\lambda,z)}{\mathrm{d}z}-\lambda^2 T(\lambda,z)=0, \tag{4}$$

where $T(\lambda, z)$ is the Hankel transform of $t(r, z)$.

The boundary condition turns to

$$\frac{\partial T(\lambda,z)}{\partial z}=F(\lambda)=-\frac{P}{2\pi k}\exp\left(-\frac{r_0^2\lambda^2}{8}\right),\ \text{at } z=0, \tag{5}$$

$$\lim_{z\to\infty}T(\lambda,z)=0, \tag{6}$$

where $F(\lambda)$ is the Hankel transform of $f(r)$.

The solution of Eq.(4) is

$$T(\lambda,z)=A(\lambda)\exp(\lambda z)+B(\lambda)\exp(-\lambda z). \tag{7}$$

With Eqs.(5) and (6), then

$$A(\lambda)=0, \tag{8}$$

$$B(\lambda)=-\frac{1}{\lambda}F(\lambda). \tag{9}$$

By taking the inverse Hankel transform, the temperature of the film sample surface is

$$t(r,0)=\frac{P}{2\pi k}\int_0^\infty J_0(\lambda r)\exp\left(-\frac{r_0^2\lambda^2}{8}\right)\mathrm{d}\lambda, \tag{10}$$

where $J_0(\lambda r)$ is the zero order Bessel function.

The average temperature of the film sample surface is

$$\begin{aligned}\hat{t}&=\frac{1}{\pi r_0^2}\int_0^{r_0}t(r,0)2\pi r\mathrm{d}r\\&=\frac{P}{\pi r_0^2 k}\int_0^{r_0}\left[\int_0^\infty J_0(\lambda r)\exp\left(-\frac{r_0^2\lambda^2}{8}\right)\mathrm{d}\lambda\right]r\mathrm{d}r\\&=\frac{\left[I_0(1)+I_1(1)\right]P}{\sqrt{2\pi}\mathrm{e}r_0 k},\end{aligned} \tag{11}$$

where $I_0(x)$ is the zero order and $I_1(x)$ is the first order modified Bessel function of the first kind.

So for the case of Gaussian laser beam irradiation, the thermal conductivity of the film sample can be expressed as

$$k=\frac{\left[I_0(1)+I_1(1)\right]P}{\sqrt{2\pi}\mathrm{e}r_0\hat{t}}. \tag{12}$$

For the micro-Raman method, $\hat{t}$ is the temperature rise induced by laser irradiation. Eq.(12) is the new basic equation for the micro-Raman method. The new basic equation can be applied to obtain the thermal conductivity of film with a thickness greater than the laser beam diameter. To obtain the thermal conductivity of film with the thickness of submicrometer- or nanometer-scale, however, the effects of thin film thickness and thermal conductivity of the substrate need to be taken into account.

Heat transfer in thin film induced by a Gaussian laser beam

Consider a sample that consists of a thick substrate with a relatively thin film. The thickness of the film is of submicrometer- or nanometer-scale. When focusing the Gaussian laser beam on the sample, the generated heat flux transfers not only within the film, but also across the film/substrate interface into the

substrate. So when applying Eq.(12) to this sample, the obtained thermal conductivity is not the film thermal conductivity, but the apparent thermal conductivity of the sample:

$$k_{\text{app}}=\frac{[I_0(1)+I_1(1)]P}{\sqrt{2\pi}\mathrm{e}r_0\hat{t}}. \tag{13}$$

Actually, k_{app} indicates a general thermal characteristic that consists of the thermal characteristics of the film, the substrate and their interface. To obtain the film effective thermal conductivity, k_{eff}, the relationship between k_{app} and k_{eff} needs to be determined.

The sample, consisting of a thin film and substrate, is at first treated as a whole. Assuming that the whole thickness of the sample is much greater than the laser beam diameter, the heat transfer process of laser irradiation of the sample can be simplified as a heat flux transfer within a semi-infinite half-space from a circular region on the surface of this half-space. The thermal conductivity of the half-space is uniform. In this case, the thermal resistance is

$$R=\frac{\Delta t}{Q}=\frac{\hat{t}}{P}=\frac{I_0(1)+I_1(1)}{\sqrt{2\pi}\mathrm{e}r_0k_{\text{app}}}. \tag{14}$$

Then, as mentioned above, because the film thickness is of submicrometer- or nanometer-scale, the heat flux transfers in the film and crosses the film/substrate interface into the substrate. Thus, the film thermal conductivity, film thickness, substrate thermal conductivity and interface thermal resistance all have effects on the heat transfer process. Those effects are reflected by the thermal resistance of the sample R. Assuming that the film thickness is much less than the substrate thickness (i.e., the substrate is relatively an infinite half-plane), then,

$$\frac{\partial^2 t_{\text{f}}(r,z)}{\partial r^2}+\frac{1}{r}\frac{\partial t_{\text{f}}(r,z)}{\partial r}+\frac{\partial^2 t_{\text{f}}(r,z)}{\partial z^2}=0, \tag{15}$$

$$\frac{\partial^2 t_{\text{s}}(r,z)}{\partial r^2}+\frac{1}{r}\frac{\partial t_{\text{s}}(r,z)}{\partial r}+\frac{\partial^2 t_{\text{s}}(r,z)}{\partial z^2}=0, \tag{16}$$

where $t_{\text{f}}(r, z)$ is the temperature in the film and $t_{\text{s}}(r, z)$ is the temperature in the substrate.

Because of the heat flux continuity,

$$t_{\text{f}}(r,z)=t_{\text{s}}(r,z),\ \text{at } z=\delta, \tag{17}$$

$$k_{\text{eff}}\frac{\partial t_{\text{f}}(r,z)}{\partial z}=k_{\text{s}}\frac{\partial t_{\text{s}}(r,z)}{\partial z},\ \text{at } z=\delta, \tag{18}$$

where k_{eff} is the effective thermal conductivity of the film, comprised of the intrinsic thermal conductivity of the film and the interface thermal resistance, and k_{s} is the thermal conductivity of the substrate.

The boundary condition at the film surface is

$$\frac{\partial t_{\text{f}}(r,z)}{\partial z}=f(r)=-\frac{I(r)}{k_{\text{eff}}}=-\frac{2P}{k_{\text{eff}}\pi r_0^2}\exp\left(-\frac{2r^2}{r_0^2}\right),\quad \text{at } 0<r<r_0,\ z=0. \tag{19}$$

It is assumed that as $(r^2+z^2)^{1/2}\to\infty$, $t_{\text{s}}(r, z)\to 0$.

Then the temperature in the film is

$$t_{\text{f}}(r,z)=\frac{P}{2\pi k_{\text{eff}}}\int_0^\infty\left[\frac{b\exp(-\lambda z)+a\exp[\lambda(z-2\delta)]}{b-a\exp(-2\lambda\delta)}\cdot J_0(\lambda r)\exp\left(-\frac{r_0^2\lambda^2}{8}\right)\right]\mathrm{d}\lambda, \tag{20}$$

where

$$a=\frac{k_{\text{eff}}-k_{\text{s}}}{2k_{\text{eff}}},\quad b=\frac{k_{\text{eff}}+k_{\text{s}}}{2k_{\text{eff}}}.$$

The average temperature of the film surface is

$$\hat{t}=\frac{1}{\pi r_0^2}\int_0^{r_0}t_{\text{f}}(r,0)2\pi r\mathrm{d}r,$$

$$=\frac{[I_0(1)+I_1(1)]P}{\sqrt{2\pi}\mathrm{e}r_0k_{\text{eff}}}+\frac{2P}{\pi r_0k_{\text{eff}}}\sum_{j=1}^{\infty}\left(\frac{a}{b}\right)^j\theta(\alpha_j), \tag{21}$$

where

$$\theta(\alpha_j)=\int_0^\infty\frac{\exp(-\alpha_j x-x^2/8)J_1(x)}{x}\mathrm{d}x,$$

$$\alpha_j=\frac{2j\delta}{r_0}.$$

α_j is small because the thickness of thin film is much less than the radius of the laser beam. $\exp(-\alpha_j x)$ can be expanded as

$$\exp(-\alpha_j x)=1+\sum_{n=1}^{\infty}\frac{(-\alpha_j x)^n}{n!}\approx 1-\alpha_j x,$$

then

$$\hat{t}=\frac{[I_0(1)+I_1(1)]P}{\sqrt{2\pi}er_0k_s}+\frac{(1-e^{-2})P}{\pi r_0 k_{eff}}\frac{\delta}{r_0}\left[1-\left(\frac{k_{eff}}{k_s}\right)^2\right]. \quad (22)$$

The thermal resistance of the sample is given by

$$R=\frac{\hat{t}}{P}=\frac{I_0(1)+I_1(1)}{\sqrt{2\pi}er_0k_s}+\frac{1-e^{-2}}{\pi r_0 k_{eff}}\frac{\delta}{r_0}\left[1-\left(\frac{k_{eff}}{k_s}\right)^2\right]. \quad (23)$$

Carslaw and Jaeger (1959) obtained the expression of R for the case of a semi-infinite half-space. Dryden (1983) obtained the expression of R in terms of δ, k_{eff} and k_s for the case of a film/substrate assembly with $f(r)=P/[2\pi k_{eff}r_0(r_0^2-r^2)^{1/2}]$. Lambropoulos *et al.*(1989) combined Carslaw and Jaeger's work and Dryden's work to evaluate the thermal conductivity of thin film using a thermal comparator method. However, the measurement uncertainty of the thermal comparator method is up to 100%, mainly because the contact area between the measurement tip and the sample cannot be correctly evaluated, and the $f(r)$ used by Dryden is not suitable as a thermal comparator.

Combining Eqs.(14) and (23), we obtain

$$\frac{k_s}{k_{app}}=1+\sqrt{\frac{2}{\pi}}\frac{e-e^{-1}}{I_0(1)+I_1(1)}\frac{\delta}{r_0}\frac{k_s}{k_{eff}}\left[1-\left(\frac{k_{eff}}{k_s}\right)^2\right]. \quad (24)$$

If the thermal conductivity of the film is much less than that of the substrate, then Eq.(24) could be simplified as

$$\frac{k_s}{k_{app}}=1+\sqrt{\frac{2}{\pi}}\frac{e-e^{-1}}{I_0(1)+I_1(1)}\frac{\delta}{r_0}\frac{k_s}{k_{eff}},$$

or

$$k_{eff}=\sqrt{\frac{2}{\pi}}\frac{e-e^{-1}}{I_0(1)+I_1(1)}\frac{\delta}{r_0}\frac{k_s k_{app}}{k_s-k_{app}}, \quad (25)$$

which indicates the relationship between k_{app} and k_{eff}.

Fig.2 indicates that when k_{eff} is one order less than k_s, it can be assumed that Eq.(25) is equivalent to Eq.(24). For the thickest film considered in Fig.2 (δ/r_0=0.1), the discrepancy between Eq.(24) and Eq.(25) is about 9% when k_{eff} equals k_s. With Eq.(25), the micro-Raman method is extended to measure the effective thermal conductivity of thin film with a thickness of submicrometer- or nanometer-scale.

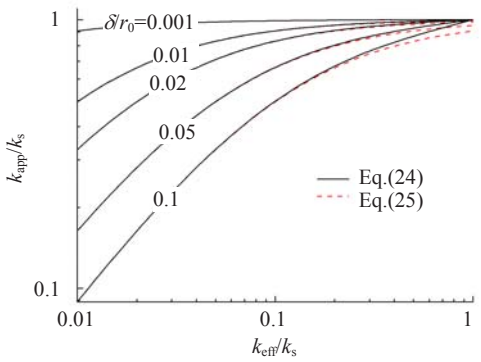

Fig.2 Comparison of the relationship between k_{eff} and k_{app} as given by Eq.(24) and Eq.(25) for several ratios δ/r_0

EXPERIMENTS

Porous silicon samples with different porosity and thickness were prepared and then tested by the micro-Raman method using the new basic equation. The effective thermal conductivities of dielectric thin film samples with submicrometer- or nanometer-scale thickness, such as silicon dioxide films and silicon nitride films, were obtained by the extended micro-Raman method.

Sample preparation and experimental setup

The porous silicon samples were prepared by electrochemical anodic etching of *p*-type, <100>-oriented, 0.01~0.05 Ω·cm silicon wafers, 525 μm thick, in solution ranging from 20% to 30% (v/v) HF, ethanol and water. The thickness of porous silicon films was measured using a KOSAKA SE3500 profile meter with an accuracy of 5 nm, after the porous silicon films were etched by dilute KOH solution. The porosity of the porous silicon samples was measured using a gravimetric method (Gesele *et al.*, 1997).

The silicon dioxide film samples were prepared by depositing the silicon dioxide films on the silicon substrates with the magnetron sputtering device at 100 °C. The silicon substrate was *p*-type, <100>-oriented, with a thickness of 525 μm and thermal conductivity of 157 W/(m·K). The thickness

of the silicon dioxide films was also measured using the profile meter.

The silicon nitride film samples were prepared by depositing the silicon nitride films on the silicon substrates in a low pressure chemical vapor deposition (LPCVD) furnace at a temperature of 850 °C. The silicon substrate was *p*-type, <100>-oriented, with a thickness of 525 μm and thermal conductivity of 157 W/(m·K).

The micro-Raman spectroscopy device used in our test was an ALMEGA (Thermo Nicolet Co., USA) with an OLYMPUS BX50 microscope. The measurement range of the Raman spectrum was 100~4000 cm^{-1}. An Ar^+-ion laser with a wavelength of 532 nm was used in our experiments. The power distribution of the laser beam had a Gaussian nature and a radius r_0 of 8 μm.

Experiments

Fig.3 shows a schematic diagram of the micro-Raman method.

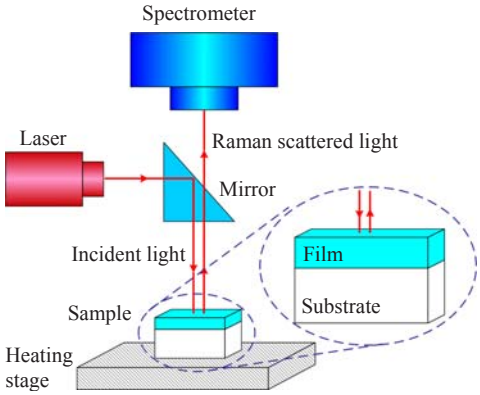

Fig.3 Schematic diagram of the micro-Raman method

In this section, we present the process of thermal conductivity measurement of porous silicon sample 1 with a porosity of 64% and a thickness of 93 μm. Porous silicon sample 1 was heated to different temperatures from 100 to 500 °C with an interval of 100 °C by using the heating stage with an accuracy of 1 °C to calibrate the relationship between the sample temperature and its Raman peak position. The heating stage was held for 1 min at each temperature to ensure that the sample was thoroughly heated. Then the Raman spectrum was acquired at each temperature while the power of the laser beam was 1.8 mW and the acquisition time was longer than 12 s. It should be noted that a low power laser beam was used in the calibration so as not to induce an additional temperature rise. The Raman peak positions of the porous silicon sample 1 at different temperatures were marked as shown in Fig.4. The relationship between the temperature and the Raman peak position of the porous silicon sample could then be calibrated as shown in Fig.5.

Fig.5 indicates a near linear relationship between the temperature and the Raman peak position of the tested sample: the Raman peak position decreases as the temperature rises. A similar linear relationship was reported by Balkanski *et al.*(1983).

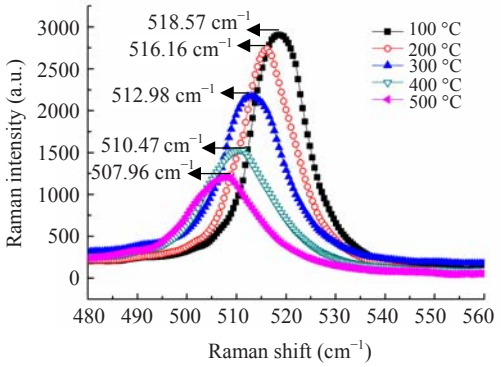

Fig.4 Raman spectra and peak positions of porous silicon sample 1 with a porosity of 64% and a thickness of 93 μm at different temperatures

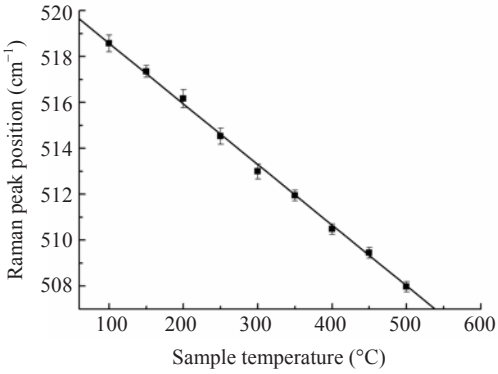

Fig.5 Raman peak position vs temperature of porous silicon sample 1 with a porosity of 64% and a thickness of 93 μm at a low laser power *P*=1.8 mW

A high power laser beam with *P*=9 mW was focused on the porous silicon sample 1 at room temperature, and the corresponding Raman spectrum was acquired. The uncertainty of the Raman peak position was estimated to be ±0.25 cm^{-1} due to the resolution of the micro-Raman spectroscopy device. The Raman

spectrum quality could be improved by enhancing the acquisition time to be longer than 12 s, enabling the Raman peak position to be acquired more accurately. By using the value of the Raman peak position induced by high power laser irradiation, the corresponding temperature value was determined (Fig.5). This corresponding temperature represented the result of local heating on porous silicon sample 1 induced by laser irradiation with power P=9 mW. Then by using the new basic equation Eq.(12), the thermal conductivity of porous silicon sample 1 could be obtained as shown in Table 1.

The thermal conductivity of porous silicon sample 1 with a porosity of 64% is 0.85 W/(m·K) (Table 1). This value is similar to the result reported by Gesele *et al.*(1997), where a thermal conductivity of 0.8 W/(m·K) was measured using the 3ω method for a meso porous silicon sample with a porosity of 64%.

Table 1 Thermal conductivity of porous silicon samples

No.	Current density (mA/cm^2)	Porosity (%)	Thickness (μm)	Thermal conductivity (W/(m·K))
1	80	64	93	0.85
2	60	53	84	2.43
3	40	37	86	5.37

The measurement process for silicon dioxide and silicon nitride film samples was similar to that for porous silicon samples. For the silicon dioxide and silicon nitride film samples, the film thickness was nanometer- or submicrometer-scale, much smaller than the silicon substrate thickness and the laser beam radius r_0. The thickness of silicon substrate was much greater than the laser beam radius r_0. The thermal conductivities k_{eff} of silicon dioxide and silicon nitride films reported in (Lee *et al.*, 1995; Lee and Cahill, 1997; Callard *et al.*, 1999) were much smaller than the thermal conductivity of silicon substrate k_s, which means that the assumptions of the extension process were all met. So the effective thermal conductivity of silicon dioxide and silicon nitride films can be obtained using the extended micro-Raman method as shown in Fig.6.

Fig.6 shows an obvious decrease in the effective thermal conductivity of the thin film with the decrease in the thickness of the silicon dioxide and silicon nitride films. The decrease in the effective thermal

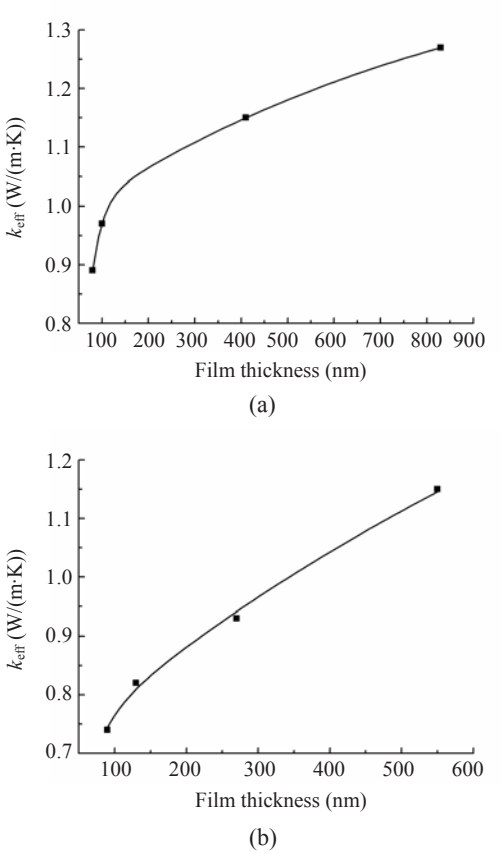

Fig.6 Variation of effective thermal conductivity of thin film with thickness for (a) silicon dioxide films and (b) silicon nitride films

conductivity is less than one order of magnitude and is similar to published results (Lee and Cahill, 1997; Burzo *et al.*, 2003). There are three possible reasons for this observed decrease in effective thermal conductivity. The first is that phonon boundary scattering of the thermal carriers reduces the thermal conductivity of the thin film. We believe that phonons with mean free paths do not cause a significant decrease of film thermal conductivity at room temperature, as claimed by many authors (Love and Anderson, 1990; Goodson *et al.*, 1994; Cahill, 1998). The second is that the microstructure and stoichiometry of the thin film changes. Internal defects such as dislocation and cracks can influence the heat transport in thin film. For the 80-nm-thick silicon dioxide thin film, we find it unlikely that internal defects can cause drastic decrease in thermal conductivity. Burzo *et al.*(2003) suspected that the difference in the microstructure of sputtered silicon dioxide film is responsible for the decrease in the effective thermal conductivity. For

LPCVD silicon nitride thin films, the internal defects are less important because dislocation is more likely healed by a process of annealing at 850 °C. The third possible reason is that thermal resistance at the interface between the thin film and the substrate can affect the effective thermal conductivity of thin film. A plausible hypothesis is the presence of a porous layer at the interface which results in heat transport reduction through the interface. To calculate the interface thermal resistance, a 1D heat flow analysis is applicable, as

$$R_{\text{eff}} = \frac{\delta}{k_{\text{eff}}} = \frac{\delta}{k_{\text{f}}} + R_{\text{i}}, \tag{26}$$

where R_{eff} is the effective thermal resistance of thin film, k_{f} is the intrinsic thermal conductivity of thin film and R_{i} is the interface thermal resistance.

Eq.(26) implies a plot of R_{eff} vs δ, which has a slope of $1/k_{\text{f}}$ and an intercept of R_{i} as shown in Fig.7.

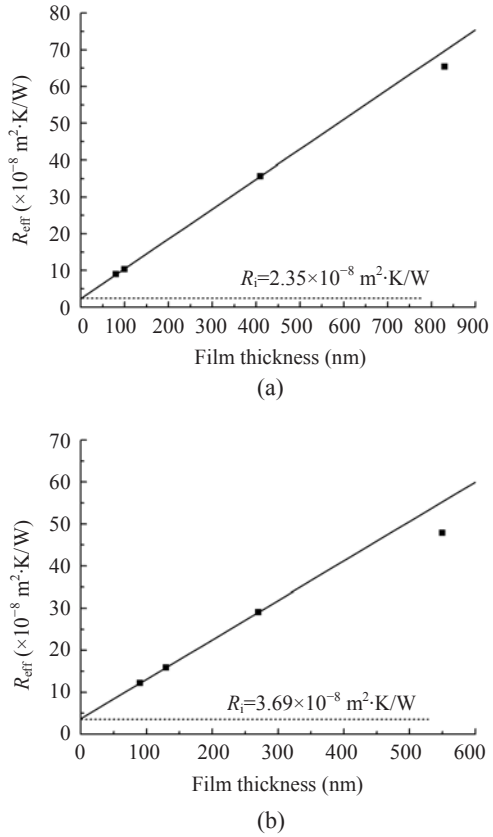

Fig.7 Variation of effective thermal resistance with thickness for (a) silicon dioxide films and (b) silicon nitride films

As shown in Fig.7, for both silicon dioxide and silicon nitride films of thickness <500 nm, a straight line can be fitted to give the value of k_{f} and R_{i}. An intrinsic film thermal conductivity of 1.23 W/(m·K) can be found in Fig.7a for silicon dioxide film. This value is in agreement with the published data. For example, Burzo *et al.*(2003) reported a thermal conductivity of 1.27 W/(m·K) for thermally grown silicon dioxide film and 1.05 W/(m·K) for ion beam sputtered silicon dioxide film; Kato and Hatta (2005) reported a thermal conductivity of (1.24±0.04) W/(m·K) using a thermo-reflectance method. The interface thermal resistance between silicon dioxide film and substrate is 2.35×10^{-8} m^2·K/W (Fig.7a). This is also similar to the value of 2.58×10^{-8} m^2·K/W for ion beam sputtered silicon dioxide film on silicon substrate according to Burzo *et al.*(2003). The intrinsic film thermal conductivity and interface thermal resistance of silicon nitride film can be found in Fig.7b to be 1.07 W/(m·K) and 3.69×10^{-8} m^2·K/W, respectively. These results are also similar to the reported data, e.g., Govorkov *et al.*(1997) found a thermal conductivity of 1.2 W/(m·K) for sputtered silicon nitride film; Lee and Cahill (1997) reported that the interface thermal resistance of a PECVD silicon nitride film on silicon substrate was about 2×10^{-8} m^2·K/W. Considering the impact of different thin film fabrication processes, some small differences in the measured thermal conductivity data are inevitable.

The main random error of the micro-Raman method is estimated to be 8% because of the ±0.25 cm^{-1} uncertainty on the Raman peak position. However, by enhancing the acquisition time, the Raman spectra quality can be improved. Systematic errors associated with the effective laser beam diameter, and heat radiation and convection will be taken into account in future, more quantitative studies.

CONCLUSION

A new basic equation has been developed for the heat source of a Gaussian laser beam to reduce the measurement error induced by a poorly fitting equation. The thermal conductivity of porous silicon has been measured using the micro-Raman method with the new basic equation.

An analytical heat transfer model has also been developed based on the new equation, by using thermal resistance to describe the effects of thin film thickness and thermal conductivity of thin film and substrate. This enables the extension of the micro-Raman method to thermal conductivity measurements of thin films with submicrometer- or nanometer-scale thickness. The extended micro-Raman method has been applied to the intrinsic thermal conductivity measurement of silicon dioxide and silicon nitride films with submicrometer- or nanometer-scale thickness. The thermal resistance of the interface between dielectric thin films and silicon substrate was also obtained. The thermal conductivity of silicon dioxide film is obtained as 1.23 W/(m·K), and the interface thermal resistance between silicon dioxide film and substrate is 2.35×10^{-8} m^2·K/W. The thermal conductivity and interface thermal resistance of silicon nitride film are 1.07 W/(m·K) and 3.69×10^{-8} m^2·K/W, respectively.

The obtained values were in agreement with previously published data thereby validating our work. The extended micro-Raman method is a non-contact, non-destructive and easy method for the measurement of thermal conductivity of both bulk material and thin film. It provides new opportunities for research into both TEMS thermally insulated structures and heat dissipation in IC.

References

Balkanski, M., Wallis, R.F., Haro, E., 1983. Anharmonic effects in light scattering due to optical phonons in silicon. *Physical Review B*, **28**(4):1928-1934. [doi:10.1103/PhysRevB.28.1928]

Bruschi, P., Piotto, M., Barillaro, G., 2006. Effects of gas type on the sensitivity and transition pressure of integrated thermal flow sensors. *Sensors and Actuators A: Physical*, **132**(1):182-187. [doi:10.1016/j.sna.2006.03.021]

Burzo, M.G., Komarov, P.L., Raad, P.E., 2002. Influence of the metallic absorption layer on the quality of thermal conductivity measurements by the transient thermoreflectance method. *Microelectronics Journal*, **33**(9):697-703. [doi:10.1016/S0026-2692(02)00052-6]

Burzo, M.G., Komarov, P.L., Raad, P.E., 2003. Thermal transport properties of gold-covered thin-film silicon dioxide. *IEEE Transactions on Components and Packaging Technologies*, **26**(1):80-88. [doi:10.1109/TCAPT.2003.811467]

Cahill, D.G., 1998. Heat transport in dielectric thin films and at solid-solid interfaces, *In*: Tien, C.L., Majumdar, A., Gerner, F. (Eds.), Microscale Energy Transport. Taylor & Francis, p.108-109.

Cahill, D.G., Katiyar, M., Abelson, J.R., 1994. Thermal conductivity of α-Si: H thin films. *Physical Review B*, **50**(9):6077-6081. [doi:10.1103/PhysRevB.50.6077]

Callard, S., Tallarida, G., Borghesi, A., Zanotti, L., 1999. Thermal conductivity of SiO_2 films by scanning thermal microscopy. *Journal of Non-Crystalline Solids*, **245**(1-3):203-209. [doi:10.1016/S0022-3093(98)00863-1]

Carslaw, H.S., Jaeger, J.C., 1959. Conduction of Heat in Solids (2nd Ed.). Oxford University Press, London, p.216.

Chen, J., Engel, J., Chen, N., Liu, C., 2005. A Monolithic Integrated Array of Out-of-plane Hot-wire Flow Sensors and Demonstration of Boundary-layer Flow Imaging. 18th IEEE International Conference on Micro Electro Mechanical Systems, Miami, Florida, USA, p.299-302. [doi:10.1109/MEMSYS. 2005.1453926]

Dominguez, D., Bonvalot, B., Chau, M.T., Suski, J., 1993. Fabrication and characterization of a thermal flow sensor based on porous silicon technology. *Journal of Micromechanics and Microengineering*, **3**(4):247-249. [doi:10.1088/0960-1317/3/4/021]

Dryden, J.R., 1983. The effect of a surface coating on the constriction resistance of a spot on an infinite half plane. *Journal of Heat Transfer*, **105**:408-410.

Gesele, G., Linsmeier, J., Drach, V., Fricke, J., Arens-Fischer, R., 1997. Temperature-dependent thermal conductivity of porous silicon. *Journal of Physics D: Applied Physics*, **30**(21):2911-2916.

Goodson, K.E., Flik, M.I., Su, L.T., Antoniadis, D.A., 1994. Prediction and measurement of thermal conductivity of amorphous dielectric layers. *Journal of Heat Transfer*, **116**(2):317-323.

Govorkov, S., Ruderman, W., Horn, M.W., Goodman, R.B., Rothschild, M., 1997. A new method for measuring thermal conductivity of thin films. *Review of Scientific Instruments*, **68**(10):3828-3834. [doi:10.1063/1.1148035]

Kaltsas, G., Nassiopoulou, A.G., 1999. Novel C-MOS compatible monolithic silicon gas flow sensor with porous silicon thermal isolation. *Sensors and Actuators A: Physical*, **76**(1-3):133-138. [doi:10.1016/S0924-4247(98)00370-7]

Kan, P.Y.Y., Finstad, T.G., 2005. Oxidation of macroporous silicon for thick thermal insulation. *Materials Science and Engineering B*, **118**(1-3):289-292. [doi:10.1016/j.mseb.2004.12.044]

Kato, R., Hatta I., 2005. Thermal conductivity measurement of thermally-oxidized SiO_2 films on a silicon wafer using a thermo-reflectance technique. *International Journal of Thermophysics*, **26**(1):179-190. [doi:10.1007/s10765-005-2365-z]

Komarov, P.L., Burzo, M.G., Kaytaz, G., Raad, P.E., 2003. Transient thermo-reflectance measurement of the thermal conductivity and interface resistance of metallised natural and isotopically-pure silicon. *Microelectronics Journal*, **34**(12):1115-1118. [doi:10.1016/S0026-2692(03)00201-5]

Lambropoulos, J.C., Jolly, M.R., Amsden, C.A., Gilman, S.E., Sinicropi, M.J., Diakomihalis, D., 1989. Thermal conductivity of dielectric thin films. *Journal of Applied*

Physics, **66**(9):4230-4242. [doi:10.1063/1.343963]

Lee, S.M., Cahill, D.G., 1997. Heat transport in thin dielectric films. *Journal of Applied Physics*, **81**(6):2590-2595. [doi:10.1063/1.363923]

Lee, S.M., Cahill, D.G., Allen, T.H., 1995. Thermal conductivity of sputtered oxide films. *Physical Review B*, **52**(1): 253-257. [doi:10.1103/PhysRevB.52.253]

Love, M.S., Anderson, A.C., 1990. Estimate of phonon thermal transport in amorphous materials above 50 K. *Physical Review B*, **42**(3):1845-1847. [doi:10.1103/PhysRevB.42.1845]

Nonnenmacher, M., Wickramasinghe, H.K., 1992. Scanning probe microscopy of thermal conductivity and subsurface properties. *Applied Physics Letters*, **61**(2):168-170. [doi:10.1063/1.108207]

Perichon, S., Lysenko, V., Remaki, B., Barbier, D., Champagnon, B., 1999. Measurement of porous silicon thermal conductivity by micro-Raman scattering. *Journal of Applied Physics*, **86**(8):4700-4702. [doi:10.1063/1.371424]

Perichon, S., Lysenko, V., Roussel, Ph., Remaki, B., Champagnon, B., Barbier, D., Pinard, P., 2000. Technology and micro-Raman characterization of thick meso-porous silicon layers for thermal effect microsystems. *Sensors and Actuators A: Physical*, **85**(1-3):335-339. [doi:10.1016/S0924-4247(00)00327-7]

Tsu, R., Hernandez, J.G., 1982. Temperature dependence of silicon Raman lines. *Applied Physics Letters*, **41**(11): 1016-1018. [doi:10.1063/1.93394]

Swimm, R.T., 1983. Photoacoustic determination of thin-film thermal properties. *Applied Physics Letters*, **42**(11):955-957. [doi:10.1063/1.93812]

Zhang, X., Gridgoropoulos, C.P., 1995. Thermal conductivity and diffusivity of free-standing silicon nitride thin films. *Review of Scientific Instruments*, **66**(2):1115-1119. [doi:10.1063/1.93812]